Organic solvent forward osmosis membranes for pharmaceutical concentration

Keng Siang Goh[a], Yunfeng Chen[a], Daniel Yee Fan Ng[a], Jia Wei Chew[b], Rong Wang[a, c, *]

[a] *Singapore Membrane Technology Centre, Nanyang Environment and Water Research Institute, Nanyang Technological University, 1 Cleantech Loop, Singapore 637141, Singapore*

[b] *School of Chemical and Biomedical Engineering, Nanyang Technological University, 62 Nanyang Drive, Singapore 637459, Singapore*

[c] *School of Civil and Environmental Engineering, Nanyang Technological University, 50 Nanyang Avenue, Singapore 639798, Singapore*

* Corresponding author. Email address: rwang@ntu.edu.sg

Abstract

A scaled-up hollow fibre thin-film composite (TFC) module was successfully developed for organic solvent forward osmosis (OSFO) application in the pharmaceutical industry. The membrane consists of cross-linked P84 polyimide substrate with a polyamide selective layer, formed via interfacial polymerisation. The performance of the lab-scale module was compared to the scaled-up module in reverse osmosis and forward osmosis modes. The results from both tests revealed that the solvent permeability of the scaled-up module decreased while its selectivity increased slightly. This might be caused by the uneven distribution of liquids during interfacial polymerisation, leading to varied membrane performance. The scaled-up module was further tested for OSFO performance using a range of PEG-400 concentrations (0.5 – 2 M) in acetone and isopropanol as draw solutions. At 2 M PEG-400 concentration, the module demonstrated high isopropanol and acetone permeability of 0.63 LMH and 13.9 LMH, respectively. Moreover, the reverse solute flux of PEG-400 in acetone and isopropanol were relatively low at 0.188 g/l and 0.153 g/l, respectively. The module was further tested for OSFO application in the pharmaceutical industry by concentrating levofloxacin in acetone, using 2 M PEG-400 as draw solution. The process was able to concentrate levofloxacin from 1,000 ppm to 16,000 ppm with very low reverse solute flux of 0.178 g/l. Therefore, this work presents a scalable TFC membrane for OSFO application in the pharmaceutical industry.

Key words:

Organic solvent forward osmosis; thin-film composite membrane fabrication; scaled-up module; concentrating levofloxacin in acetone.

1. Introduction

In the pharmaceutical industry, a large portion of capital is spent on operating separation processes such as distillation for solvent swaps, dewatering and crystallisation of active pharmaceutical ingredients (APIs) [1-6]. As such, there is an economic incentive for the industry to look for alternative technology to replace current energy-consuming ones. The main challenge of finding a separation technology suitable for pharmaceutical industry is that it requires a robust process that can attain high product purity and yield [1, 3-5]. In addition, the process should not alter or contaminate the solvent stream due to the sensitive nature of the manufacturing process. Given these stringent criteria, organic solvent forward osmosis (OSFO) process has recently been touted as a potential replacement or augmentation of existing separation processes in the pharmaceutical industry [7-11]. Through recent studies, OSFO has been demonstrated to be able to operate in organic solvent environments such as ethanol, hexane, dimethylacetamide (DMAc) and dimethylformamide (DMF) [7-11]. In addition, the membranes showed excellent selectivity for low molecular weight solutes (<500 Da), which is required for pharmaceutical applications.

There are several advantages of using OSFO in various pharmaceutical manufacturing processes. Compared to existing separation processes such as distillation, the lack of thermal input in OSFO can potentially result in significantly lower energy consumption [12]. Moreover, thermally sensitive compounds like APIs will not be damaged by this separation process [2]. Another benefit rendered by OSFO is that a suitable draw solution can be used to generate sufficiently high osmotic pressure to concentrate APIs to high concentrations, which is difficult to achieve with pressure-driven membrane processes such as organic solvent nanofiltration (OSN) due to the excessively high operating pressure required to overcome the osmotic pressure. Furthermore, OSFO operates at none or low hydraulic pressure, leading to lower

external concentration polarisation [13, 14]. However, as OSFO is still an emerging field, there are numerous challenges that need to be addressed moving forward.

The challenges for OSFO process include several folds, one of which is associated with existing issues of forward osmosis (FO). Most notably, dilutive internal concentration polarisation (ICP) and reverse solute diffusion are the key issues that continue to impair the performance of osmotically-driven processes. Therefore, attempts have been extensively focused on addressing these issues in the past decade and research on OSFO can build on existing knowledge [12, 13, 15-18]. On the other hand, the introduction of a wide variety of solvents and solutes poses new challenges for researchers in the field of OSFO. Commonly used polymers for making the substrates of thin-film composite FO membranes such as polyethersulfone (PES) [14, 15, 19], polysulfone (PSf) [20, 21] and polyvinylidene fluoride (PVDF) [22] have limited chemical stability in harsh organic solvents such as DMAc and DMF. The excessive swelling or even dissolution of the polymer makes it unsuitable for OSFO applications [23]. Another potential challenge is related to the solution properties of the solute-solvent system. Solution properties such as viscosity, diffusivity and osmotic coefficients are important parameters that influence the performance of osmotically-driven membrane processes [17, 18]. This implies that the performances across different solute-solvent systems in OSFO cannot be easily compared. Another issue with current OSFO studies is that small membrane coupons of less than 10 cm^2 were normally used for performance tests [7-9, 11]. The performances of lab-scale coupons and scaled-up modules can be drastically different [24, 25]. This is especially relevant in osmotically-driven processes such as OSFO, where module design has significant impacts on liquid flow at the shell side, potentially affecting solvent permeation [16, 25].

This work aims to develop a new type of OSFO membrane and address some of the issues pertaining to OSFO. A solvent resistant thin-film composite hollow fibre membrane was developed for OSFO. Cross-linked P84 polyimide was chosen as the substrate due to its excellent solvent resistance to various organic solvents [24, 26-28]. The fabrication of the substrate was optimised to improve its structural parameter, thickness and porosity, which are key parameters to consider when fabricating a high-performance FO membrane [15, 29]. A polyamide active layer was applied on the lumen of the substrate through interfacial polymerisation (IP) to enhance the selectivity of the membrane. Lab-scale and scaled-up modules were fabricated and subjected to conventional reverse osmosis (RO) and FO tests to evaluate the impact of scaling up on membrane performance. The lab-scale and scaled-up modules possess effective membrane areas of 22 cm^2 and 4,145 cm^2, respectively. Subsequently, the OSFO performance of the scaled-up module was evaluated using a non-toxic draw solute (PEG-400) in various organic solvents. A model API, levofloxacin (361 Da in molecular weight (MW)), in acetone was concentrated using the OSFO membrane to demonstrate the feasibility of OSFO process for pharmaceutical concentration.

2. Experimental

2.1 Materials and chemicals

Polyimide (P84 Lenzing) was used to fabricate the substrate. 1-Methyl-2-pyrrolidinone (NMP, >99%) purchased from Merck and diethylene glycol (DG, >99.5%) purchased from Sigma Aldrich were used in the phase inversion process. Isopropanol (IPA, >99.5%), polyethylene glycol 400 (PEG-400) and hexamethylene diamine (HDA, >98%) purchased from Sigma Aldrich were used for post-treatment and storage of membranes. For the IP

reaction, m-phenylenediamine (MPD, >99%, Sigma Aldrich), cyclohexane (>99%, VWR) and benzene tricarbonyl trichloride (TMC, >98%, Sigma Aldrich) were used.

To evaluate the selectivity of the TFC membranes, rose bengal (1017 Da in MW, >95%, Sigma Aldrich), methyl red (269 Da in MW, Sigma Aldrich), magnesium chloride hexahydrate (>99%, Merck), sodium chloride (>99%, Merck) and levofloxacin (361 Da in MW, >98%, Sigma Aldrich) were used. Deionized (DI) water, acetone (>95%, Sigma Aldrich), ethanol (>99.5%, Sigma Aldrich) and isopropanol (>99.5%, Sigma Aldrich) were used as solvents.

2.2 Fabrication of thin-film composite hollow fibre membranes

The hollow fibre substrates were fabricated via dry-jet wet spinning process. The dope was prepared in a similar manner described in the previous work [24], but the dope composition and spinning parameters were changed as illustrated in Table 1, to improve its performance for use as FO substrate. The substrate was then cross-linked by immersing it into a solution of 20 g/l of HDA in IPA for 18 hours to achieve solvent resistance. The cross-linked membranes were then stored in 40/60 wt% PEG-400/IPA solution to preserve the pores. The fibres were subsequently potted into modules with dimensions as shown in Table 2.

Table 1: Spinning parameters of hollow fibre substrate

	This work	Previous work [24]
Dope composition P84/DG/NMP (wt%)	16/8/76	20/8/72
Dope flow rate (ml/min)	3	3.5
Bore fluid	DI water	DI water
Bore fluid flow rate (ml/min)	3	3.5
External coagulant	Tap water	Tap water
Air gap (cm)	<1	5
Drum speed (cm/s)	6	3.75

Table 2: Dimensions of module for hollow fibre FO membranes

Module	Number of Fibres	Module length (cm)	Module diameter (inch)	Membrane Area (cm^2)
P5	5	26	~ 3/8	22
P500	500	50	~ 2	4145

A polyamide selective layer was synthesized on the lumen side of the fibres through interfacial polymerisation. The MPD aqueous solution containing 1.3 wt% MPD and 0.12 wt% sodium dodecyl sulfate, and TMC solution with a concentration of 0.15 wt% in cyclohexane were prepared for the selective layer formation in the experiments. Depending on the module size (i.e., the number of fibers packed in the module, P5 or P500), a small variation in concentration of the MPD and TMC solutions was adjusted in order to achieve better performance. The membranes were first soaked in an aqueous solution containing MPD and then purged with cyclohexane to remove excess aqueous solution. Subsequently, a cyclohexane solution containing TMC was pumped through the lumens to initiate the IP reaction, forming a thin polyamide layer on the substrate. Afterwards, the reaction was quenched and the modules were stored in DI water before use.

2.3 Membrane characterisation and performance evaluation

The chemical and physical properties of the hollow fibre substrate and the selective layer were examined using a series of standardised characterisation tests. The cross-section and surface morphologies of the polyimide substrate and TFC membrane were examined using Zeiss EVO 50 Scanning Electron Microscope (SEM). The prepared hollow fibre samples were coated with platinum using EMITECH SC7620 sputter coater for the SEM preparation.

To evaluate the cross-linking of the polyimide substrate, Fourier Transform Infrared Spectroscopy (FTIR) was carried out using Prestige-21 spectrophotometer from Shimadzu. Polyimide bands at 1780 cm^{-1} and 1711 cm^{-1} (C=O), 1361 cm^{-1} (C-N), and amide bands at 1634 cm^{-1} (C=O) and 1525 cm^{-1} (C-N) of the pristine and cross-linked substrate were compared to evaluate the changes in the polymer structure. The porosity (ε) of the hollow fibre substrate can be determined by gravimetric method [30]. The inner surface of the TFC membrane was examined by X-ray photoelectron spectroscopy (XPS) using a Kratos AXIS Ultra to confirm the presence of polyamide layer after IP.

A crossflow setup was used to test the membrane in RO mode. The permeability of water, ethanol and acetone for the polyimide substrate and TFC membranes was evaluated by pressurizing the solvents from the lumen side at 2 bar. A crossflow velocity of 0.6 m/s was used. Measurements were taken after the system has stabilised and the performance were calculated using equation (1):

$$J_i = \frac{m_i}{\Delta P \times A \times \rho_i \times t} \quad (1)$$

where J_i (l m^{-2} hr^{-1} bar^{-1}) is the solvent permeability, m_i is the mass of solvent collected, ΔP (bar) is the transmembrane pressure, A (m^2) is the effect area of the membrane, ρ_i (g cm^{-3}) is the density of solvent, and t (h) is the time taken for permeate collection.

The molecular weight cut-off (MWCO) of the substrate was evaluated using standardised test with a dextran aqueous solution [31]. The selectivity of the TFC membrane was determined using aqueous salt solutions consisting of 2000 ppm NaCl and $MgCl_2$. 50 ppm of rose bengal and methyl red dissolved in ethanol and acetone, separately, were used to investigate its OSN performance. The concentrations of salts and dyes were determined using a conductivity meter (Myron L Company, Canada) and UV-1650 PC UV–Vis spectrophotometer (Shimadzu, Japan), respectively [26, 32]. The rejection (R) of dextran, salts and dyes were determined using equation (2):

$$R = \frac{C_f - C_p}{C_f} \times 100 \quad (2)$$

where C_f and C_p are the concentrations of the solutes in the feed and permeate, respectively.

A bench-scale FO setup was utilized to study the FO performance of the TFC membranes in the active layer facing feed solution (AL-FS) orientation, as shown in Figure 1. Solutions with 0.5 – 1.5 M $MgCl_2$ were used as draw solutions while DI water was used as the feed.

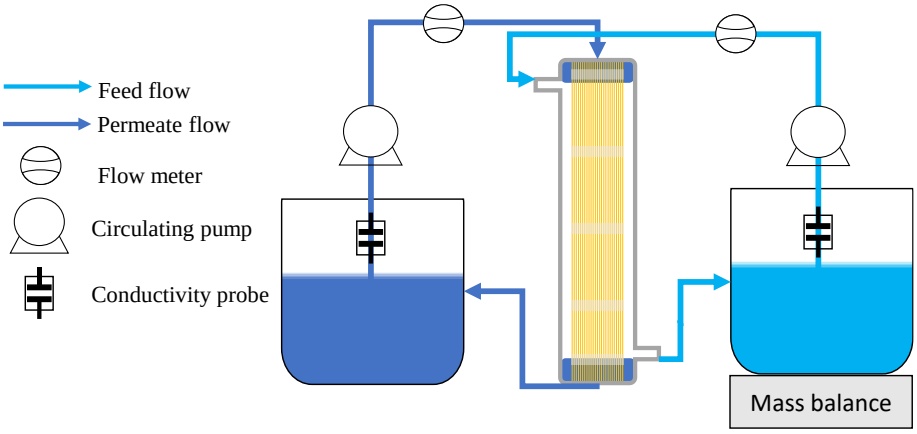

Figure 1: Schematic diagram of forward osmosis experimental setup

To determine the FO performance, the water flux J_w, (l m^{-2} hr^{-1}, LMH) was determined using equation (3):

$$J_w = \frac{\Delta w}{A_m \rho_w \Delta t} \quad (3)$$

where Δw (g) is the change in feed mass over a time interval Δt (h), A_m (m^2) is the effective membrane area and ρ_w (g/l) is the density of water.

The reverse solute flux (RSF), J_s, (g m^{-2} hr^{-1}, gMH) was examined according to equation (4):

$$J_s = \frac{C_t V_t - C_0 V_0}{A_m \Delta_t} \quad (4)$$

where C_0 (g/l) and V_0 (l) are solute concentration and feed volume at time 0, C_t and V_t indicate the final solute concentration and feed volume over a time interval (Δt), respectively. Subsequently, the specific RSF (J_s/J_w), (g/l), was plotted against draw solution concentration. The performance of P5 and P500 modules were then compared to evaluate the scalability of the TFC membrane.

The structural parameter (S) of the TFC membrane was then measured using equation (5):

$$S = \frac{D_s}{J_w} \ln \left[\frac{A\pi_D + B}{A\pi_F + J_w + B} \right] \quad (5)$$

where D_s is the diffusion coefficient for $MgCl_2$, approximated to 1.06 x 10^{-9} m^2 s^{-1} [33], Π_D is the osmotic pressure of the bulk draw solution, Π_F is the osmotic pressure of the feed solution at the membrane surface. A and B are the pure water and salt permeability coefficients, respectively.

2.4 Organic solvent forward osmosis application

The scaled-up (P500) module was tested for OSFO performance in the AL-FS orientation. The setup illustrated in Figure 1 was used for the OSFO experiments by replacing the fittings and tubes with solvent resistant ones. IPA and acetone were used as solvents and the respective solvent fluxes were measured using 0.5 – 2 M PEG-400 as draw solutions. PEG-400 concentrations in the feed and draw solutions were measured using total organic carbon (TOC) analyser (Shimadzu, Japan). A known volume of solution containing PEG-400 was first oven dried at 60ºC to completely remove the solvent and then diluted with water for TOC analysis. The solvent fluxes, RSF and specific RSF were measured similarly as described in section 2.3. A concentric cylinder (CC-27) rheometer from Anton Paar was used to examine the viscosities of the draw solutions. A shear rate (τ) of 2000 s^{-1} was used to obtain the values.

To demonstrate the OSFO capability of the P500 module, a solution of levofloxacin in acetone was concentrated. 2 M PEG-400 in acetone was used as the draw solution while 1000 ppm levofloxacin dissolved in 6 l of acetone was used as the feed solution. The feed and draw solutions were circulated in the AL-FS orientation and the draw solution was constantly dosed to maintain its concentration. The concentration of levofloxacin in the feed was determined

using UV-1650 PC UV–Vis spectrophotometer (Shimadzu, Japan) at a wavelength of 292 nm [34]. The solution was appropriately diluted before measuring to obtain an accurate reading.

3. Results and discussion

3.1 Characterisation of polyimide substrate

P84 polyimide hollow fibre substrate was spun in-house and cross-linked with HDA to achieve organic solvent resistance. The MWCO of the cross-linked substrate was then determined to be about 90 kDa using a dextran standard solution. Subsequently, the physical properties of the membrane after cross-linking were measured and shown in Table 3. Compared to the substrate fabricated in the previous work, the inner diameter, outer diameter and thickness of the membrane were significantly reduced. This was achieved by reducing the polymer concentration in the dope and increasing the uptake speed of the drum [29]. The lower polymer concentration reduces the viscosity of the dope solution, thereby having a less pronounced die swelling at the exit of the spinneret. The higher drum uptake speed also increased the elongation of the fibre, further reducing the fibre dimension. In addition, the decrease in bore and dope flow rates also contributed to a thinner fibre obtained for this study [35, 36].

Table 3: Physical properties of polyimide substrate before and after cross-linking

	This work	**Previous work [24]**
Inner diameter (μm)	573.7 ± 8.7	640.5 ± 5.2
Outer diameter (μm)	823.6 ± 10.8	920.4 ± 12.3
Thickness (μm)	125.0 ± 4.1	139.9 ± 7.7
Porosity (%)	79	68

The morphology of the cross-linked substrate was also examined using SEM imaging as shown in Figure 2. It can be observed that a thin skin layer (Figure 2 (c & e)) was formed on the outer and inner surfaces of the membrane through rapid phase inversion via using hard bore fluid and external coagulant [15, 36]. The thin skin layer allows for a defect-free polyamide selective layer to be synthesized onto the surface while reducing the overall intrinsic membrane resistance for higher solvent permeability [20, 37]. It can also be seen that the finger-like structures developed extensively towards the centre of the membrane, separated by a sponge-like polymer matrix as shown in Figure 2 (b). This was achieved by using a hard bore fluid and lower air gap (see Table 1) [15, 36]. The extensive finger-like structures resulted in an increase in porosity from 68% to 79%. Consequently, the thinner and more porous membrane would improve the structural parameter of the membrane and reduce the effects of ICP [15, 38]. Overall, the fabricated hollow fibre substrate showed desirable characteristics of a FO membrane.

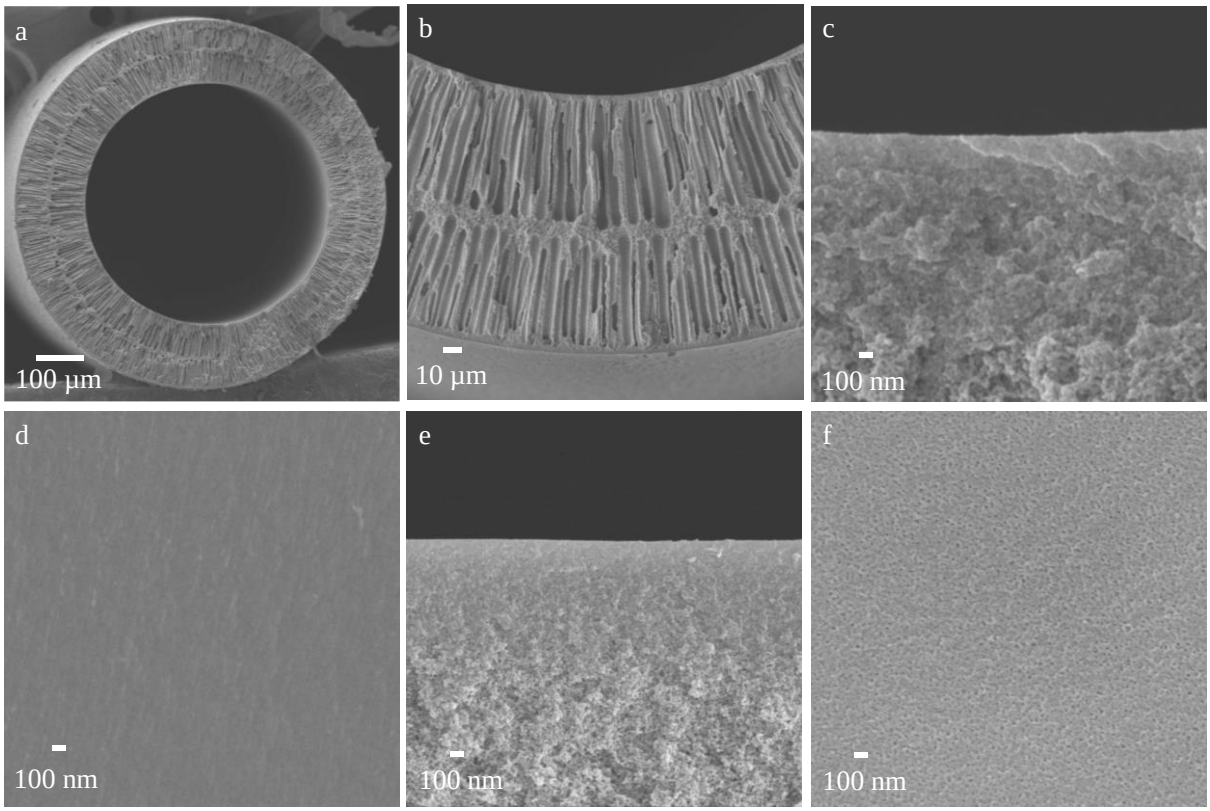

Figure 1: SEM images of cross-linked hollow fibre substrate. (a) Cross-section; (b) enlarged cross-section; (c) cross-section of inner surface; (d) inner surface; (e) cross-section of outer surface; (f) outer surface

Figure 3 illustrates the solvent permeability of the membrane fabricated in this study and the previous work [24]. It was found that the solvent permeability of the membrane fabricated in this work is much higher than that obtained from the previous work. The permeability for water, ethanol and acetone improved by about 61%, 79% and 91%, respectively. The improvements were mainly attributed to the reduction in membrane thickness and the increase in the porosity of the hollow fibre substrate. Overall, the substrate fabricated in this work showed significant improvement in its physical properties that are potentially beneficial in FO process.

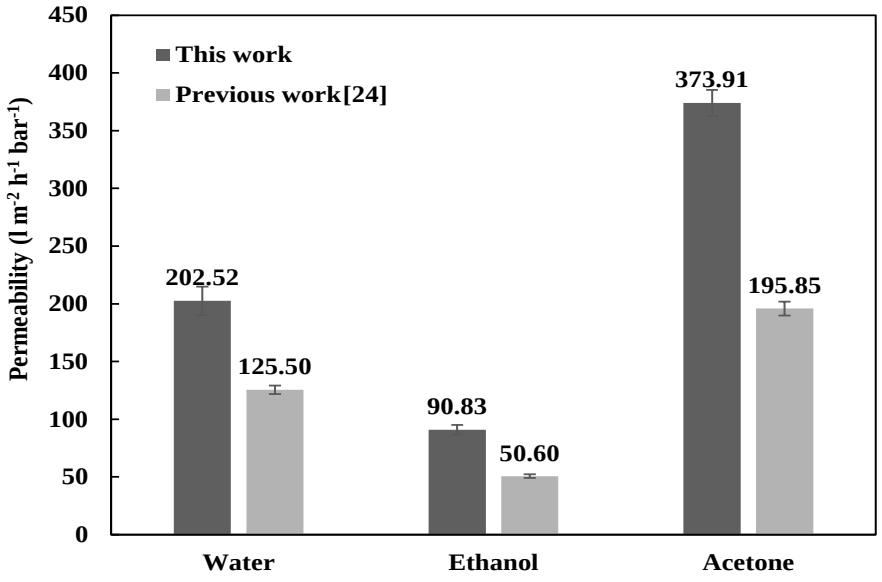

Figure 3: Solvent permeability of hollow fibre substrates in various solvents. (Operating pressure: 2 bar, crossflow velocity: 0.6 m/s)

The chemical composition of the substrate before and after cross-linking were also analysed by FTIR as presented in Figure 4. The characteristic peaks of imide groups at 1361 cm^{-1} (C=O), 1711 cm^{-1} (C=O) and 1780 cm^{-1} (C-N) diminished significantly after cross-linking. On the other hand, the amide peaks, 1634 cm^{-1} (C=O) and 1525 cm^{-1} (C-N), became more intense through the formation of amide bonds. These observations are consistent with previous works and thus, the solvent resistance of the fabricated substrate should perform similarly [24, 26]. The hollow fibre substrate was potted into two types of modules, P5 and P500, and used for subsequent experiments.

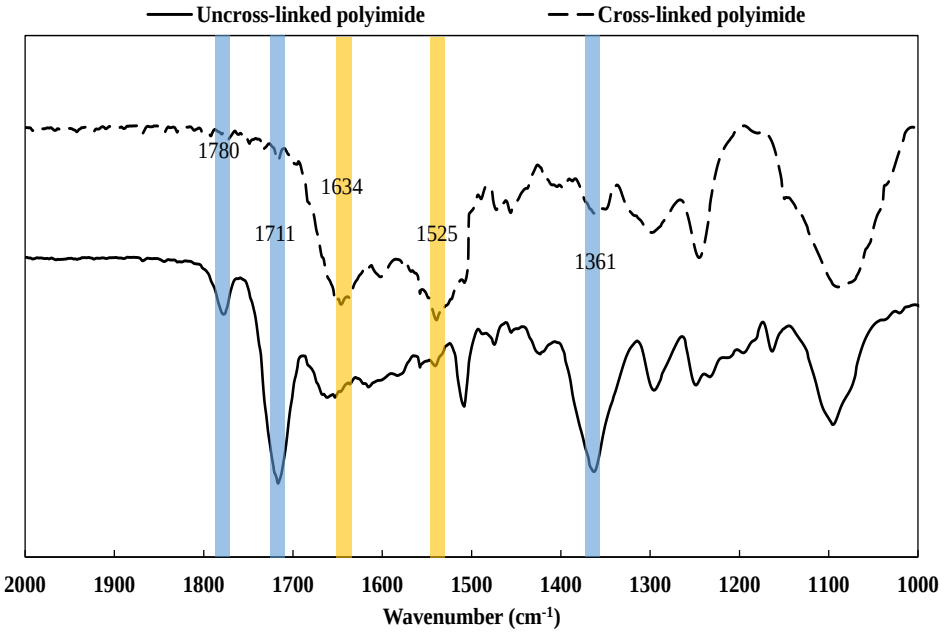

Figure 4: FTIR spectrum of uncross-linked and cross-linked polyimide substrates.

3.2 Characterisation of the selective layer

A polyamide selective layer was synthesized on the lumens of the hollow fibre substrates in P5 and P500 modules via interfacial polymerisation. The SEM images in Figure 5 show the morphology of the inner surface and cross-section of the membrane after IP. As observed in

Figure 5 (a), the inner surface of the membrane was covered by a ridge-and-valley like texture, the characteristic of a typical MPD-based polyamide layer. Looking at Figure 5 (c), the cross-section shows a selective layer thickness of about 150 nm. A thinner selective layer could potentially improve solvent permeability. However, as the OSFO membrane was used to concentrate high value pharmaceutical products, a TFC membrane with higher selectivity was favoured.

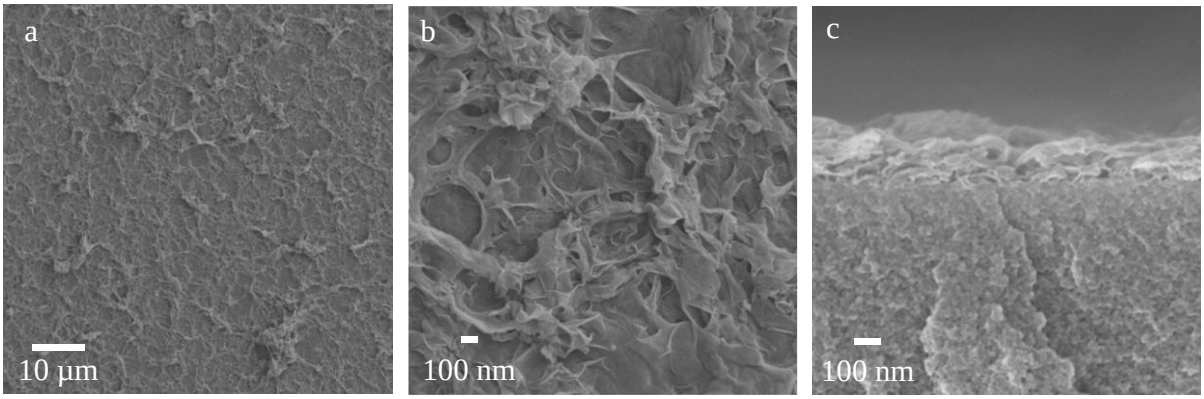

Figure 5: SEM images of thin-film composite hollow fibre membranes, (a) inner surface; (b) enlarged inner surface; (c) cross-section

The changes in surface chemistry of the membrane after IP were analysed using XPS. The N1s and O1s peaks of the polyimide substrate and TFC were deconvoluted respectively and illustrated in Figure 6. As observed from Figure 6 (a and b), the amide bonds increased after the selective layer was synthesized onto the substrate. From Figure 6 (c and d), it can also be seen that the deconvoluted O1s peaks for the membrane changed. The C=O peak of the substrate was no long present and a new O=C-O peak was detected. These observations were also made in previous works and thus suggests that the polyamide selective layer was successfully synthesized onto the substrates [24, 26].

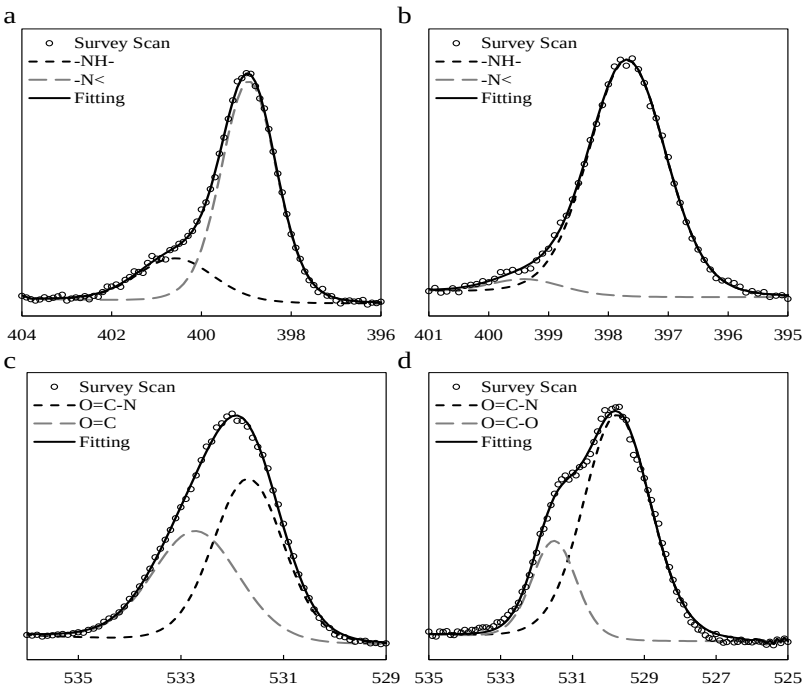

321

322 Figure 6: XPS spectra of (a) substrate N1s, (b) TFC N1s, (c) substrate O1s and (d) TFC O1s

323 The OSN performance of P5 and P500 TFC modules were evaluated using a cross-flow setup
324 and the results are illustrated in Figure 7 and Figure 8, respectively. Ethanol permeability of
325 P5 module was measured at 1.65 l m^{-2} hr^{-1} bar^{-1} while the corresponding permeability for P500
326 module was lower at 1.04 l m^{-2} hr^{-1} bar^{-1}. This trend is similar to that reported in the previous
327 work, where the scaled-up membrane suffered from lower solvent permeability due to possible
328 non-uniform IP layer coating [24]. The increase in module length (from 30 cm to 50 cm) and
329 enlarged module cross-sectional area (from 3/8 inch to 2 inch) might have caused uneven
330 distribution of liquids during the IP process and formed less ideal selective layer. On the other
331 hand, the selectivity of P500 module was very similar to P5 module, which indicates that the
332 selective layer was synthesized onto the membrane without any defects. As observed from
333 Figure 8, P500 module showed slightly higher salt rejections of $MgCl_2$ and NaCl at 99.1% and
334 95.4%, respectively. The membranes also achieved excellent methyl red rejection of over 92%.
335 This suggests that the selective layer can serve well as a RO-like barrier for small solutes in
336 FO operation.

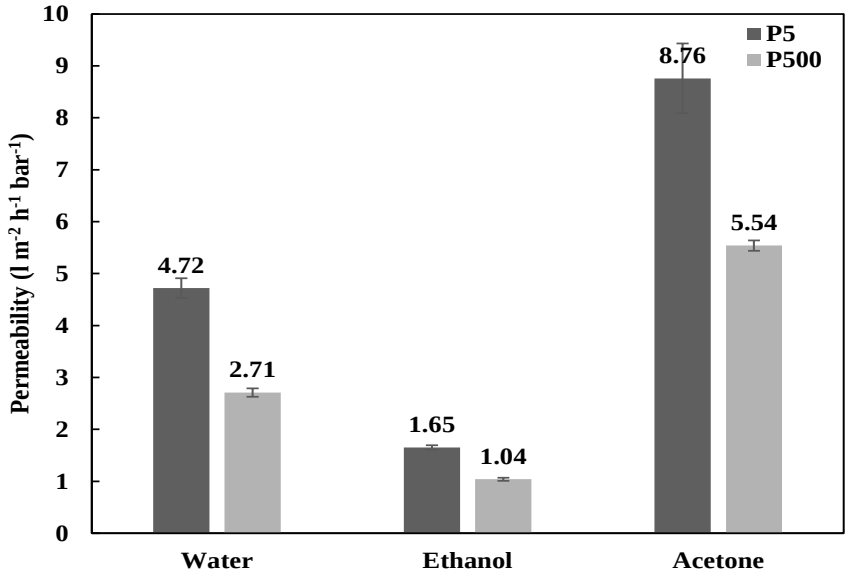

337

338 Figure 7: Solvent permeabilities for P5 and P500 thin-film composite modules in various

339 solvents (Operating pressure: 2 bar, crossflow velocity: 0.6 m/s)

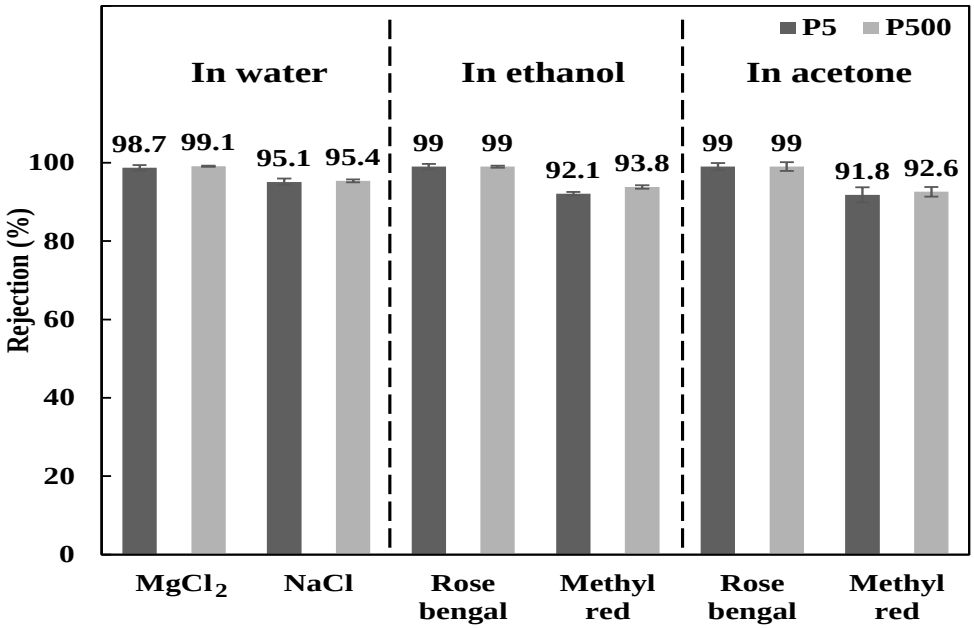

340

341 Figure 8: Solute rejections of P5 and P500 modules in various solvents (Operating pressure: 2

342 bar, crossflow velocity: 0.6 m/s)

343

3.3 FO performance of lab-scale and scaled-up modules

The modules were tested for their FO performances in the AL-FS orientation using the setup illustrated in Figure 1. Varied concentrations of $MgCl_2$ were used as the draw solution while DI water was used as the feed solution. The water flux (J_w), RSF (J_s) and calculated specific RSF (J_s/J_w) were obtained and reported in Figure 9. As seen from Figure 9 (a), the water flux of P5 module increased from 25.6 LMH to 42.9 LMH when the concentration of $MgCl_2$ in the draw solution increased from 0.5 M to 1.5 M. On the other hand, P500 module achieved water flux of 23.0 LMH and 33.2 LMH when 0.5 M and 1.0 M of $MgCl_2$ was used (Figure 9 (A)). The comparatively lower J_w of P500 module can be attributed to its relatively lower intrinsic water permeability than P5 module, which is expected from the solvent permeability test in Figure 7. It can also be observed from Figure 9 (a) that there is a diminishing increase in flux when the concentration of draw solution further increased. This suggests that dilutive ICP is much more noticeable at a higher concentration of draw solution [39, 40]. As seen from Figure 9 (b and B), the estimated specific RSF of P5 module was higher than P500 module. This suggests that the polyamide layer synthesized on P500 module was more selective than that on P5 module. This observation can also be verified by the higher solute rejections as illustrated in Figure 8. Nevertheless, both P5 and P500 modules exhibited excellent selectivity with very low specific RSF values. It is interesting to see that the specific RSFs of P5 and P500 modules at 0.5 M, 1.0 M and 1.5 M $MgCl_2$ draw solutions were relatively constant. This phenomenon is consistent with several FO studies, where the specific RSF was found to be independent of the concentration of draw solution [40, 41]. Overall, the performance of the membrane in FO mode demonstrated consistent trends with that reported in RO mode.

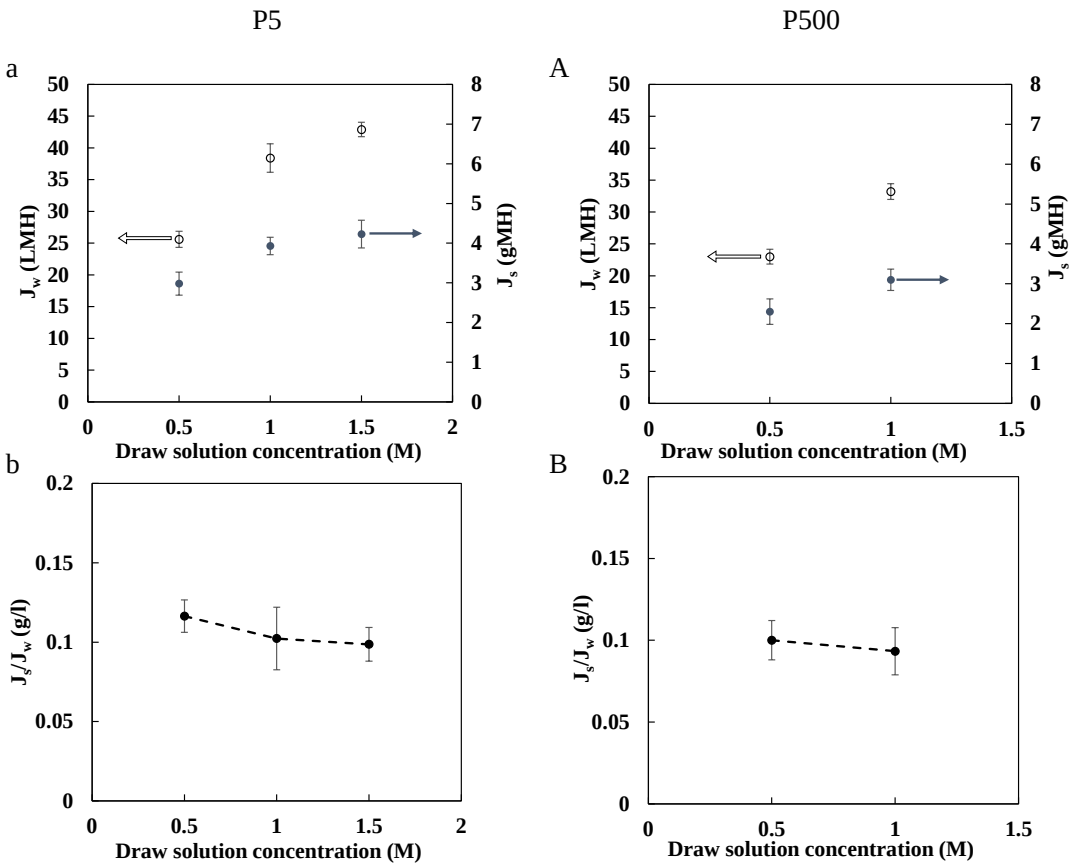

Figure 9: FO performance of P5 and P500 modules in AL-FS orientation. (a) and (A) Water flux (Jw) and RSF (Js); (b) and (B) Specific RSF (Js/Jw)

3.4 OSFO performance tests for P500 module

The organic solvent forward osmosis performance of P500 module was evaluated with a number of solvents and draw solutions. 0.5 – 2M of PEG-400 were used as draw solutes to investigate acetone and IPA fluxes of the module in the AL-FS orientation. Figure 10 illustrates the solvent fluxes and RSF when varied concentrations of draw solution were used. As observed from Figure 10 (a), the acetone flux increased steadily from 5.1 LMH to 13.9 LMH when the concentration of PEG-400 draw solution increased from 0.5 M to 2 M. The RSF of PEG-400 also increased as a function of draw solution concentration. This phenomenon is in line with that observed in recent studies on OSFO [9, 11]. In addition, this observation is also similar to that obtained in the FO study, which suggests that the solute transport mechanism

for OSFO is similar to FO process [42]. From Figure 10 (A), the IPA flux and RSF also increased with increasing concentration of draw solution. However, IPA fluxes (0.22 LMH to 0.63 LMH) were much lower than acetone even though the same concentrations of draw solutions were used. This is consistent with OSN experiments, where ethanol and IPA were reported to have much lower permeability than acetone [24, 26]. One possible explanation is that IPA has significantly higher viscosity (8.15 mPa.s) compared to acetone (2.24 mPa.s) as shown in Table 4. The hydrophilic membrane also has a higher affinity to the more polar acetone [43]. In addition, the difference in Hansen solubility parameter (R_a) of acetone to the substrate (5.04 $MPa^{0.5}$) is smaller than IPA to the substrate (11.57 $MPa^{0.5}$), which also contributed to a comparatively higher mass transport of acetone [44].

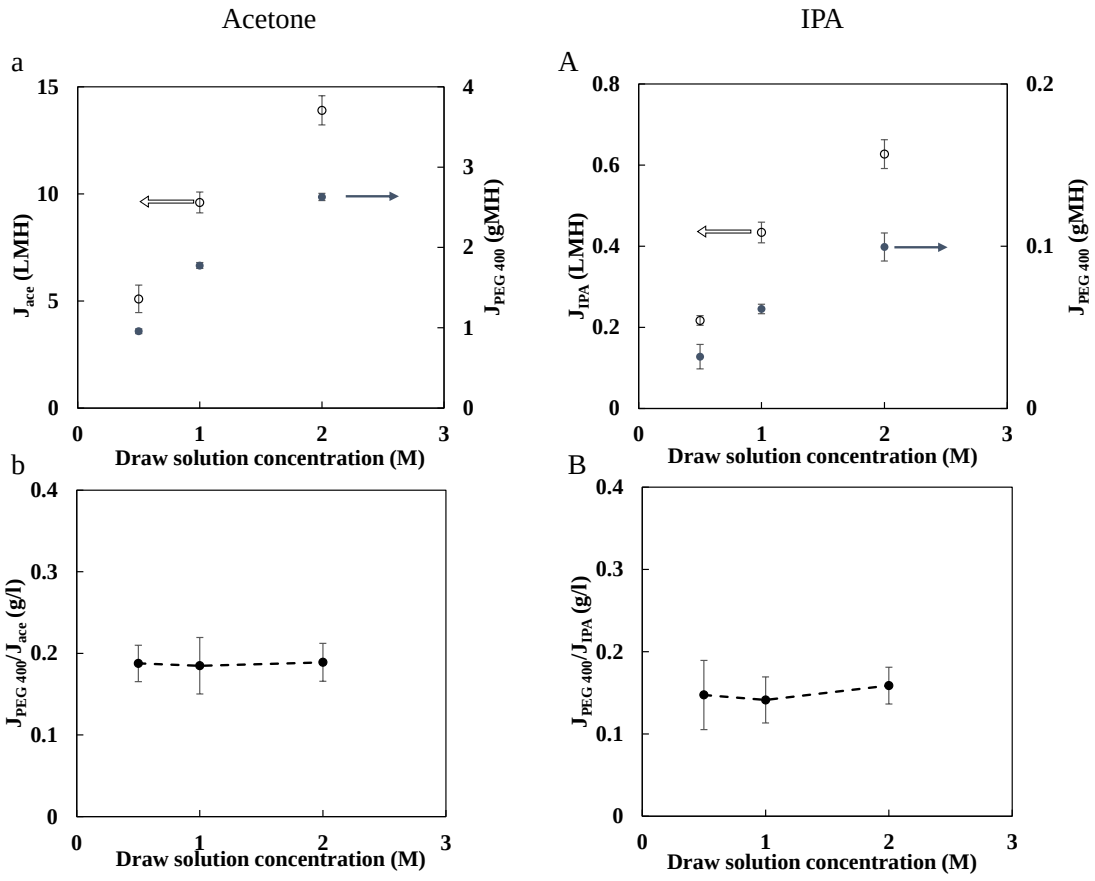

Figure 10: Effect of draw solution concentration on organic solvent forward osmosis performance. (a) Acetone flux (J_{ace}) and RSF ($J_{PEG\ 400}$); (A) IPA flux (J_{IPA}) and RSF ($J_{PEG\ 400}$); (b) and (B) Specific solute flux of PEG-400

Table 4: Viscosity of different solutions

Solvent	Draw solute	Viscosity (mPa.s)
Acetone	Pure solvent	2.24
	0.5 M PEG-400	4.79
	1 M PEG-400	7.70
	2 M PEG-400	20.0
IPA	Pure solvent	8.15
	0.5 M PEG-400	13.1
	1 M PEG-400	17.8
	2 M PEG-400	26.3

The solvent flux and RSF also increased at a diminishing rate as the concentrations of draw solutions increased. This is even more apparent when IPA was used as the solvent. As the membrane was tested in the AL-FS orientation, this suggests that there were significant ICP occurring when higher concentrations of draw solutions were used [39]. This might be caused by substantially higher viscosities of the draw solutions when higher concentrations of PEG-400 were used, as shown in Table 4. The increase in viscosity can potentially inhibit the diffusion of the bulk draw solution into the substrate due to a thicker boundary layer, which resulted in a more severe ICP phenomenon [17, 45]. As shown in Figure 10 (b and B), the specific RSF of PEG-400 in acetone (~0.1877 g/l) is higher than IPA (~0.1527 g/l). Since specific RSF is an intrinsic parameter of the selective layer, this indicates that the selectivity of the membrane changed in different organic solvents. One possible explanation is that acetone caused the substrate and selective layer to swell slightly, which reduced its selectivity

409 [46]. Similar observations were made in a previous OSN study, where solute rejections of
410 Starmem^{TM} 122 and Puramem^{TM} 280 were dependent on the extent of membrane swelling and
411 solute solubility parameter in the particular solvent [47]. Studies have also shown that the
412 diffusivity of solutes are influenced by solvent properties [48, 49]. Consequently, the type of
413 solvent used in a draw solution will affect the reverse solute diffusion [41, 42]. This finding
414 suggests a new challenge for OSFO research such that the performance obtained for different
415 solute-solvent systems might not be comparable, adding to the complexity of reviewing
416 literature for analysis.
417
418 The P500 module was subsequently used to concentrate levofloxacin using 2 M PEG-400 as
419 draw solution. Acetone was used as solvent for both the feed and draw solutions. The solvent
420 flux and RSF were plotted against feed concentration as illustrated in Figure 11. The initial
421 levofloxacin feed of 1000 ppm was gradually concentrated to approximately 16,000 ppm, a
422 concentration factor of about 16. As observed from Figure 11 (a), the initial acetone flux is
423 slightly lower than that when pure acetone was used as feed. It also decreased at an increasing
424 rate when the feed got more concentrated. This might be caused by the increase in severity of
425 concentrative external concentration polarisation (ECP), where levofloxacin built up on the
426 membrane surface at the feed side [39, 41]. This phenomenon can be diminished by increasing
427 the cross-flow velocity of the feed stream, thereby reducing the effect of ECP on OSFO
428 performance. Studies have also shown that an FO membrane with high permeate flux can
429 intensify the phenomenon of ECP [16, 39]. Thus, a draw solution with lower osmotic pressure
430 can be used to minimize this effect. Similarly, the RSF decreased as the concentration of feed
431 gradually increased. This is expected as RSF is proportional to solvent flux [41, 42]. From
432 Figure 11 (b), the specific RSF stayed relatively constant when the feed was gradually
433 concentrated. This implies that this parameter is independent of external factors such as feed

concentration and draw solution concentrations. Instead, it was shown to be dependent on the intrinsic selectivity of the membrane for a particular solute-solvent system [41, 42].

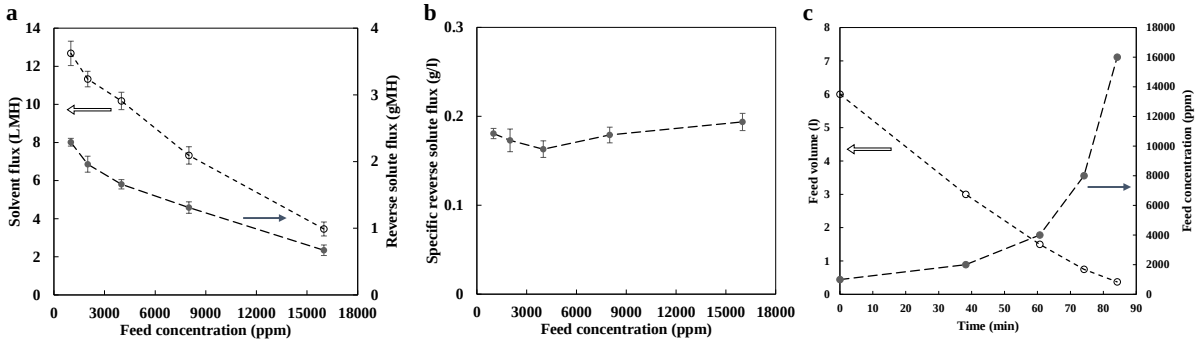

Figure 11: Concentration of levofloxacin in AL-FS orientation. Effects of feed concentration on (a) solvent and RSF; (b) specific RSF; (c) Change in feed volume and feed concentration

The levofloxacin concentration process was listed together with existing membrane-based concentration experiments in solute-solvent systems reported in literature (Table 5). As publications on OSFO applications are very limited, the concentration applications by OSN were also included for illustration. From the table, the closest reference that could be made is an OSFO study by Chung et al [9]. In the study, tetracycline (444 Da in molecular weight) dissolved in ethanol was concentrated from 1000 ppm to 10,000 ppm using 2 M LiCl as draw solution. On the other hand, the OSFO study conducted in current work concentrated levofloxacin (361 Da in molecular weight) in acetone to a concentration of 16,000 ppm, showing promising performance of this process. However, it is clear that OSFO is still at a very early stage of study. The real feeds in pharmaceutical industry are much more sophisticated than single solute-solvent systems, which pose great challenges to OSFO for practical application. Thus, future work should focus on testing OSFO membranes with a feed that closely resembles the pharmaceutical feed streams. Likewise, the challenge of draw solution regeneration should also be addressed in order for OSFO systems to be competitive to existing purification processes.

455 Table 5: Concentrating feed in solvent streams using membrane-based separation processes

Process	Feed system	Driving force	Feed concentration	Final concentration	Ref Year
3-stage OSN	Rosmarinic acid in ethanol	20 – 40 bar	0.118 g/l	0.346 g/l	[50] 2011
2-stage OSN	Roxithromycin in methanol	30 bar	~ 120 ppm	~ 210 ppm	[51] 2014
OSFO	Tetracycline in ethanol	2 M LiCl in ethanol	1000 ppm	10,000 ppm	[9] 2018
OSN	Levofloxacin in acetone	<10 bar	500 ppm	20,000 ppm	[24] 2021
OSFO	Levofloxacin in acetone	2 M PEG-400 in acetone	1000 ppm	16,000 ppm	This work

456

4. Conclusions

In this work, a scaled-up thin-film composite hollow fibre membrane module with a membrane surface area of 4,145 cm^2 was developed for organic solvent forward osmosis process. The spinning parameters and dope composition used for membrane substrate fabrication were optimised to decrease the mass transport resistance of the substrate with high porosity and low structural parameter. Subsequently, a polyamide selective layer was synthesized on the lumen of the substrate. The following conclusions can be made via this study:

- The resultant P500 module showed promising OSFO results with high IPA and acetone fluxes of 0.63 LMH and 13.9 LMH, respectively, using 2 M PEG-400 as draw solute.
- The membrane achieved low specific RSF using PEG-400 as draw solute for both solvent systems, which indicated that the selectivity was maintained in both organic solvent environments.
- Levofloxacin in acetone was concentrated with 2 M PEG-400 as draw solution using P500 module. A concentration factor of 16 can be achieved while maintaining high selectivity.

This study demonstrated promising potential of OSFO to be used in the pharmaceutical industry for API concentration. Further studies should focus on using feeds with compositions similar to real pharmaceutical feeds to evaluate the feasibility of using OSFO process in the pharmaceutical industry. In addition, identifying suitable draw solutes for the myriad of solute-solvent combinations present in the pharmaceutical industry is also an important task.

Acknowledgements

The authors acknowledge Economic Development Board (EDB) of Singapore for funding the Singapore Membrane Technology Centre (SMTC), Interdisciplinary Graduate Programme, Nanyang Environment and Water Research Institute, Nanyang Technological University.

5. References

[1] M.G. Buonomenna, J. Bae, Organic Solvent Nanofiltration in Pharmaceutical Industry, Separation & Purification Reviews, 44 (2015) 157-182.

[2] J. Geens, B. De Witte, B. Van der Bruggen, Removal of API's (active pharmaceutical ingredients) from organic solvents by nanofiltration, Separation Science and Technology, 42 (2007) 2435-2449.

[3] K. Grodowska, A. Parczewski, Organic solvents in the pharmaceutical industry, Acta poloniae pharmaceutica, 67 (2010) 3-12.

[4] J. Vanneste, D. Ormerod, G. Theys, D. Van Gool, B. Van Camp, S. Darvishmanesh, B. Van der Bruggen, Towards high resolution membrane-based pharmaceutical separations, Journal of Chemical Technology & Biotechnology, 88 (2013) 98-108.

[5] S.D. Schaber, D.I. Gerogiorgis, R. Ramachandran, J.M.B. Evans, P.I. Barton, B.L. Trout, Economic Analysis of Integrated Continuous and Batch Pharmaceutical Manufacturing: A Case Study, Industrial & Engineering Chemistry Research, 50 (2011) 10083-10092.

[6] P. Marchetti, M.F. Jimenez Solomon, G. Szekely, A.G. Livingston, Molecular separation with organic solvent nanofiltration: A critical review, Chemical Reviews, 114 (2014) 10735-10806.

[7] Z. Zhou, Y. Hu, Q. Wang, B. Mi, Carbon nanotube-supported polyamide membrane with minimized internal concentration polarization for both aqueous and organic solvent forward osmosis process, Journal of Membrane Science, 611 (2020) 118273.

[8] Z. Tong, H. Guo, X. Liu, B. Zhang, Organic Solvent Forward Osmosis of Graphene Oxide-Based Membranes for Enrichment of Target Products, Industrial & Engineering Chemistry Research, 59 (2020) 19012-19019.

[9] Y. Cui, T.-S. Chung, Pharmaceutical concentration using organic solvent forward osmosis for solvent recovery, Nature Communications, 9 (2018) 1426.

[10] X. Wu, M. Ding, H. Xu, W. Yang, K. Zhang, H. Tian, H. Wang, Z. Xie, Scalable Ti3C2Tx MXene Interlayered Forward Osmosis Membranes for Enhanced Water Purification and Organic Solvent Recovery, ACS Nano, 14 (2020) 9125-9135.

[11] Y. Wei, Y. Wang, L. Wang, H. Yang, H. Jin, P. Lu, Y. Li, Simultaneous phase-inversion and crosslinking in organic coagulation bath to prepare organic solvent forward osmosis membranes, Journal of Membrane Science, 620 (2021) 118829.

[12] D.L. Shaffer, J.R. Werber, H. Jaramillo, S. Lin, M. Elimelech, Forward osmosis: Where are we now?, Desalination, 356 (2015) 271-284.

[13] T.Y. Cath, A.E. Childress, M. Elimelech, Forward osmosis: Principles, applications, and recent developments, Journal of Membrane Science, 281 (2006) 70-87.

[14] R. Wang, L. Shi, C.Y. Tang, S. Chou, C. Qiu, A.G. Fane, Characterization of novel forward osmosis hollow fiber membranes, Journal of Membrane Science, 355 (2010) 158-167.

[15] L. Shi, S.R. Chou, R. Wang, W.X. Fang, C.Y. Tang, A.G. Fane, Effect of substrate structure on the performance of thin-film composite forward osmosis hollow fiber membranes, Journal of Membrane Science, 382 (2011) 116-123.

[16] J.R. Mccutcheon, M. Elimelech, Modeling water flux in forward osmosis: Implications for improved membrane design, AIChE Journal, 53 (2007) 1736-1744.

[17] S. Zhao, L. Zou, Relating solution physicochemical properties to internal concentration polarization in forward osmosis, Journal of Membrane Science, 379 (2011) 459-467.

[18] W.C.L. Lay, J. Zhang, C. Tang, R. Wang, Y. Liu, A.G. Fane, Factors affecting flux performance of forward osmosis systems, Journal of Membrane Science, 394-395 (2012) 151-168.

[19] S. Chou, L. Shi, R. Wang, C.Y. Tang, C. Qiu, A.G. Fane, Characteristics and potential applications of a novel forward osmosis hollow fiber membrane, Desalination, 261 (2010) 365-372.

[20] N.Y. Yip, A. Tiraferri, W.A. Phillip, J.D. Schiffman, M. Elimelech, High Performance Thin-Film Composite Forward Osmosis Membrane, Environmental Science & Technology, 44 (2010) 3812-3818.

[21] J. Wei, C. Qiu, C.Y. Tang, R. Wang, A.G. Fane, Synthesis and characterization of flat-sheet thin film composite forward osmosis membranes, Journal of Membrane Science, 372 (2011) 292-302.

[22] M. Tian, C. Qiu, Y. Liao, S. Chou, R. Wang, Preparation of polyamide thin film composite forward osmosis membranes using electrospun polyvinylidene fluoride (PVDF) nanofibers as substrates, Separation and Purification Technology, 118 (2013) 727-736.

[23] E.J. Kappert, M.J.T. Raaijmakers, K. Tempelman, F.P. Cuperus, W. Ogieglo, N.E. Benes, Swelling of 9 polymers commonly employed for solvent-resistant nanofiltration membranes: A comprehensive dataset, Journal of Membrane Science, 569 (2019) 177-199.

[24] K.S. Goh, Y. Chen, J.Y. Chong, T.H. Bae, R. Wang, Thin film composite hollow fibre membrane for pharmaceutical concentration and solvent recovery, Journal of Membrane Science, 621 (2021) 119008.

[25] Y. Chen, C.H. Loh, L. Zhang, L. Setiawan, Q. She, W. Fang, X. Hu, R. Wang, Module scale-up and performance evaluation of thin film composite hollow fiber membranes for pressure retarded osmosis, Journal of Membrane Science, 548 (2018) 398-407.

[26] K.S. Goh, J.Y. Chong, Y. Chen, W. Fang, T.-H. Bae, R. Wang, Thin-film composite hollow fibre membrane for low pressure organic solvent nanofiltration, Journal of Membrane Science, 597 (2020) 117760.

[27] C. Li, S. Li, L. Lv, B. Su, M.Z. Hu, High solvent-resistant and integrally crosslinked polyimide-based composite membranes for organic solvent nanofiltration, Journal of Membrane Science, 564 (2018) 10-21.

[28] H. Mariën, I.F.J. Vankelecom, Transformation of cross-linked polyimide UF membranes into highly permeable SRNF membranes via solvent annealing, Journal of Membrane Science, 541 (2017) 205-213.

[29] X. Li, C.H. Loh, R. Wang, W. Widjajanti, J. Torres, Fabrication of a robust high-performance FO membrane by optimizing substrate structure and incorporating aquaporin into selective layer, Journal of Membrane Science, 525 (2017) 257-268.

[30] C. Feng, R. Wang, B. Shi, G. Li, Y. Wu, Factors affecting pore structure and performance of poly(vinylidene fluoride-co-hexafluoro propylene) asymmetric porous membrane, Journal of Membrane Science, 277 (2006) 55-64.

[31] S. Mochizuki, A.L. Zydney, Dextran transport through asymmetric ultrafiltration membranes: Comparison with hydrodynamic models, Journal of Membrane Science, 68 (1992) 21-41.

[32] W. Fang, L. Shi, R. Wang, Interfacially polymerized composite nanofiltration hollow fiber membranes for low-pressure water softening, Journal of Membrane Science, 430 (2013) 129-139.

[33] D.G. Miller, J.A. Rard, L.B. Eppstein, J.G. Albright, Mutual diffusion coefficients and ionic transport coefficients lij of magnesium chloride-water at 25.degree.C, The Journal of Physical Chemistry, 88 (1984) 5739-5748.

[34] M. Maleque, M.R. Hasan, F. Hossen, S. Safi, Development and validation of a simple UV spectrophotometric method for the determination of levofloxacin both in bulk and marketed dosage formulations, Journal of Pharmaceutical Analysis, 2 (2012) 454-457.

[35] J. Qin, T.-S. Chung, Effect of dope flow rate on the morphology, separation performance, thermal and mechanical properties of ultrafiltration hollow fibre membranes, Journal of Membrane Science, 157 (1999) 35-51.

[36] M. Rahbari-sisakht, A.F. Ismail, T. Matsuura, Effect of bore fluid composition on structure and performance of asymmetric polysulfone hollow fiber membrane contactor for CO2 absorption, Separation and Purification Technology, 88 (2012) 99-106.

[37] A. Tiraferri, N.Y. Yip, W.A. Phillip, J.D. Schiffman, M. Elimelech, Relating performance of thin-film composite forward osmosis membranes to support layer formation and structure, Journal of Membrane Science, 367 (2011) 340-352.

[38] B. Kim, G. Gwak, S. Hong, Review on methodology for determining forward osmosis (FO) membrane characteristics: Water permeability (A), solute permeability (B), and structural parameter (S), Desalination, 422 (2017) 5-16.

[39] J.R. McCutcheon, M. Elimelech, Influence of concentrative and dilutive internal concentration polarization on flux behavior in forward osmosis, Journal of Membrane Science, 284 (2006) 237-247.

[40] C.Y. Tang, Q. She, W.C.L. Lay, R. Wang, A.G. Fane, Coupled effects of internal concentration polarization and fouling on flux behavior of forward osmosis membranes during humic acid filtration, Journal of Membrane Science, 354 (2010) 123-133.

[41] C. Suh, S. Lee, Modeling reverse draw solute flux in forward osmosis with external concentration polarization in both sides of the draw and feed solution, Journal of Membrane Science, 427 (2013) 365-374.

[42] W.A. Phillip, J.S. Yong, M. Elimelech, Reverse Draw Solute Permeation in Forward Osmosis: Modeling and Experiments, Environmental Science & Technology, 44 (2010) 5170-5176.

[43] S. Darvishmanesh, A. Buekenhoudt, J. Degrève, B. Van der Bruggen, General model for prediction of solvent permeation through organic and inorganic solvent resistant nanofiltration membranes, Journal of Membrane Science, 334 (2009) 43-49.

[44] S. Araki, D. Gondo, S. Imasaka, H. Yamamoto, Permeation properties of organic compounds from aqueous solutions through hydrophobic silica membranes with different functional groups by pervaporation, Journal of Membrane Science, 514 (2016) 458-466.

[45] M. Xie, W.E. Price, L.D. Nghiem, M. Elimelech, Effects of feed and draw solution temperature and transmembrane temperature difference on the rejection of trace organic contaminants by forward osmosis, Journal of Membrane Science, 438 (2013) 57-64.

[46] E. Dražević, K. Košutić, V. Freger, Permeability and selectivity of reverse osmosis membranes: Correlation to swelling revisited, Water Research, 49 (2014) 444-452.

[47] P. Schmidt, T. Köse, P. Lutze, Characterisation of organic solvent nanofiltration membranes in multi-component mixtures: Membrane rejection maps and membrane selectivity maps for conceptual process design, Journal of Membrane Science, 429 (2013) 103-120.

[48] T. Chan, I. Lee, K. Chan, Effect of Solvent on Diffusion: Probing with Nonpolar Solutes, The Journal of Physical Chemistry B, 118 (2014) 10945-10955.

[49] A.J. Easteal, L.A. Woolf, Solute–solvent interaction effects on tracer diffusion coefficients, Journal of the Chemical Society, Faraday Transactions 1: Physical Chemistry in Condensed Phases, 80 (1984) 1287-1295.

[50] D. Peshev, L.G. Peeva, G. Peev, I.I.R. Baptista, A.T. Boam, Application of organic solvent nanofiltration for concentration of antioxidant extracts of rosemary (Rosmarinus officiallis L.), Chemical Engineering Research and Design, 89 (2011) 318-327.

[51] L. Peeva, J.d.S. Burgal, I. Valtcheva, A.G. Livingston, Continuous purification of active pharmaceutical ingredients using multistage organic solvent nanofiltration membrane cascade, Chemical Engineering Science, 116 (2014) 183-194.